Analysis of Echoes from a Solid Elastic Sphere in Water

ROBERT HICKLING
California Institute of Technology, Pasadena, California

(Received May 3, 1962)

It is well known in sonar work that the pulse form of a direct echo from a target bears little relation to the form of the original signal. This is true even for regularly shaped bodies, such as a sphere. In this paper, the case of a homogeneous elastic sphere in water is examined theoretically and it is shown in comparison with experimental results, that the observed effects originate from vibrations induced in the sphere by the incident sound. Calculated results are presented for a variety of solid materials and it seems that echo forms could possibly provide information about the size and constitution of a sonar target.

1. INTRODUCTION

IT is well known in sonar work that the pulse form of the direct echo returned by a stationary insonified target in water is usually quite different from that of the original signal sent out by the transducer. This effect can be observed even when the target has a regular shape as in the case of a sphere. In the experiments which have been made, the incident sound has consisted of single-frequency constant-amplitude pulses of various lengths, and the echo pulse generally appears in the form of multiple echoes of the original pulse; i.e., compared to the original pulse, the echo is generally longer and subject to amplitude modulation. Presumably there are also differences in frequency content, but there does not appear to be any quantitative data available on the subject.

If the body has an irregular shape it is possible to suppose that this effect is due to echoes returned by the individual irregularities. However, in the case of regularly shaped bodies with no abrupt changes in curvature, such an explanation cannot be used. In this event it would seem reasonable to suppose that the distortion in the echo is caused either by diffraction or by vibrations occurring within the solid material of the target or by both. The frequencies used in sonar usually preclude the influence of diffraction, so that the observed effects would appear to be due mainly to vibrations in the solid. Since the density of any solid does not differ from that of water by much more than a factor of 8, it seems quite possible for the incident sound to cause vibrations in the solid material of the target. In air the corresponding density ratio would be of the order of 10^4 so that a target would react more like a rigid body, with a consequent diminution in echo distortion.

It is the purpose of this paper to test the validity of this hypothesis in the case of a homogeneous solid sphere supporting shear and compressional waves. Suitable experimental data[1] have recently become available and these are compared with calculated results based on known formal solutions.[2,3] These results were obtained using a high-speed computer. Previous calculations have been made for fluid[4] and rigid[5] spheres.

2. FORMULATION OF THE PROBLEM

The coordinate system for the sphere is shown in Fig. 1, where the relationship between the Cartesian and spherical polar coordinates is

$$x=r\sin\theta\cos\phi, \quad y=r\sin\theta\sin\phi, \quad z=r\cos\theta. \tag{1}$$

The sphere is assumed to consist of solid isotropic material supporting both compressional and shear waves having velocities c_1 and c_2, respectively. Outside the sphere there is a limitless fluid of density ρ and sound velocity c in which there is a continuous train of waves emanating from a point source situated on the z axis at $r=r_0$, $\theta=\pi$. The time dependence of these waves is of the form $\exp(-i\omega t)$ from which the wavenumber k in the fluid is obtained by means of the relation

$$k=\omega/c=2\pi/\lambda,$$

where λ is the wavelength. Similar relations

$$k_1=\omega/c_1 \quad \text{and} \quad k_2=\omega/c_2$$

hold for the compressional and shear waves in the solid. The waves emanating from the point source can be expressed[6] as

$$p_i=P_0\exp(ikD)/D$$

$$=ikP_0\sum_{n=0}^{\infty}(2n+1)(-1)^nP_n(\cos\theta)j_n(kr)h_n(kr_0) \qquad (0<r<r_0), \tag{2}$$

where

$$D=(r_0^2+2rr_0\cos\theta+r^2)^{\frac{1}{2}}$$

and the P_n are Legendre polynomials, and the j_n, h_n are spherical Bessel functions.[7] Plane waves incident on the sphere are obtained by making r_0 go to infinity. Using

[1] L. D. Hampton and C. M. McKinney, J. Acoust. Soc. Am. 33, 664 (1961).
[2] J. J. Faran, J. Acoust. Soc. Am. 23, 405 (1951).
[3] P. M. Morse and H. Feshbach, *Methods of Theoretical Physics* (McGraw-Hill Book Company, Inc., New York, 1953), Vol. II, p. 1483.
[4] V. C. Anderson, J. Acoust. Soc. Am. 22, 426 (1950).
[5] H. Stenzel, *Leitfaden zur Berechnung von Schallvorgagen* (Springer-Verlag, Berlin, 1939).
[6] Reference 3, p. 1466.
[7] Reference 3, p. 1325 and p. 1573.

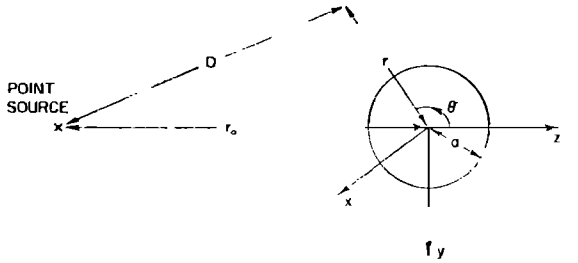

FIG. 1. Coordinate system.

the two limits

$$\exp(ikD)/D \to \exp(ikr_0)\exp(ikr\cos\theta)/r_0,$$
$$h_n(kr_0) \to i^{-(n+1)}\exp(ikr_0)/kr_0, \qquad (3)$$

and removing the common factor $\exp(ikr_0)/r_0$ gives

$$p_i = P_0\exp(ikr\cos\theta)$$
$$= P_0\sum_{n=0}^{\infty}(2n+1)i^n P_n(\cos\theta)j_n(kr). \qquad (4)$$

The above waves p_i incident on the sphere result in scattered waves in the fluid which will be of the form

$$p_s = P_0\sum_{n=0}^{\infty}c_n h_n(kr)P_n(\cos\theta). \qquad (5)$$

The coefficients c_n have to be determined from the appropriate boundary conditions at the surface of the sphere and can be shown[8] to be

$$c_n = k(-1)^n(2n+1)h_n(kr_0)\sin\eta_n\exp(-i\eta_n), \qquad (6)$$

where the angle η_n is given by

$$\tan\eta_n = -[j_n(x)F_n - j_n'(x)]/[n_n(x)F_n - n_n'(x)] \qquad (7)$$

with

$$F_n = \frac{\rho}{\rho_1}\frac{x_2^2}{2}\frac{\dfrac{x_1 j_n'(x_1)}{x_1 j_n'(x_1)-j_n(x_1)} - \dfrac{2(n^2+n)j_n(x_2)}{(n^2+n-2)j_n(x_2)+x_2^2 j_n''(x_2)}}{x_1^2\{[\sigma/(1-2\sigma)]j_n(x_1)-j_n''(x_1)\} - \dfrac{2(n^2+n)[j_n(x_2)-x_2 j_n'(x_2)]}{(n^2+n-2)j_n(x_2)+x_2^2 j_n''(x_2)}}{x_1 j_n'(x_1)-j_n(x_1)} \qquad (8)$$

and

$$x = ka; \quad x_1 = k_1 a; \quad x_2 = k_2 a.$$

The primes denote the derivative with respect to the argument. This result was first derived by Faran.[2] However, there was an error in his presentation in which the factor $\sigma/(1-2\sigma)$ was misplaced. Finally it should be noted that the expression on the right-hand side of Eq. (6) is of the form $f(x)/[f(x)+ig(x)]$, where f and g are regular on the real axis. Hence there are no singularities when the argument is real, and the function can be integrated numerically in a straightforward manner. It also follows that the solution as presented is complete for all frequencies, i.e., the boundary conditions are fully satisfied by the shear and compressional waves already postulated.

Certain limiting cases are of interest. If $F_n \to 0$, the solution would then apply to scattering by a rigid immovable sphere.[4] This would be the case for instance when the density of the solid was very much greater than that of the fluid. If $F_n \to \infty$ the solution for scattering by a free-surface sphere is obtained.[9] This corresponds to the condition where the normal stress at the surface of the sphere vanishes, which would result for example when the density of the material inside the sphere was very much less than that of the fluid.

From the above it follows that the echo returned by the solid sphere to the source is given by

$$p_e = \frac{P_0}{2r_0}\left[-2x_0\sum_{n=0}^{\infty}(2n+1)\sin\eta_n \times\exp(-i\eta_n)h_n^2(x_0)\right]\exp(-i\omega t)$$
$$= (P_0/2r_0)f(x,x_0,x_1,x_2)\exp(-ix\tau), \qquad (9)$$

where $x_0 = kr_0 = xR$, and $\tau = ct/a$. When the source is a large distance from the sphere,

$$p_e = \frac{P_0 a}{2r_0^2}\left[\frac{2}{x}\sum_{n=0}^{\infty}(-1)^n(2n+1)\sin\eta_n \times\exp(-i\eta_n)\right]\exp[ik(2r-ct)]$$
$$= (P_0 a^2/2r_0^2)f_e(x,x_1,x_2)\exp[ix(2R-\tau)]. \qquad (10)$$

Removal of a factor $\exp(ikr_0)/r_0$ gives the solution for incident plane waves. Equations (9) and (10) can then be used to construct the echo due to a pressure pulse emanating from the source. Suppose the source emits a pulse of form $P_e(t)$. This can be expressed in terms of Fourier components as

$$P_e(t) = \frac{P_0 c}{(2\pi)^{1/2}D}\int_{-\infty}^{\infty}g(k)\exp[ik(D-ct)]dk, \qquad (11)$$

[8] P. M. Morse, *Vibration and Sound* (McGraw-Hill Book Company, Inc., New York, 1948), p. 354.
[9] Reference 3, p. 1483.

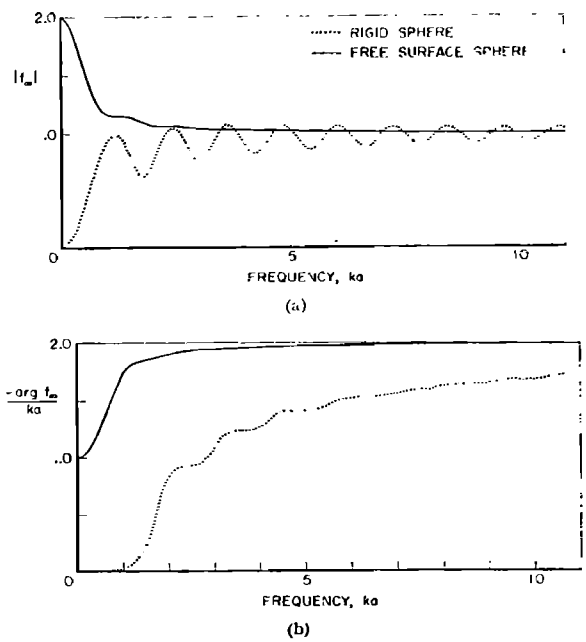

FIG. 2 (a). The pressure amplitude as a function of frequency of the echo returned by rigid and free-surface spheres to a distant source of continuous waves. (b) The phase of the echo from rigid and free surface spheres as a function of frequency.

where D is as defined previously. The frequency spectrum $g(k)$ is found by taking the Fourier transform of the given pulse, i.e.,

$$g(k)=\frac{1}{(2\pi)^{\frac{1}{2}}}\int_{-\infty}^{\infty}P_i(t)\exp[-ik(D-ct)]dt. \quad (12)$$

With the new variable $x=ka$, the reflected pulse will be

$$P_e(\tau)=\frac{P_0c}{(2\pi)^{\frac{1}{2}}ar_0}\int_{-\infty}^{\infty}g(x)f(x,x_0,x_1,x_2)\exp(-ix\tau)dx, \quad (13)$$

and when the point source moves to a large distance from the sphere,

$$P_r(\tau)=\frac{P_0}{2(2\pi)^{\frac{1}{2}}r_0^2}\int_{-\infty}^{\infty}g(x)f_\infty(x,x_1,x_2)\times\exp[ix(2R-\tau)]dx. \quad (14)$$

In general the echo given by (14) will differ in form from that of the incident pulse (11). Only for high frequencies in the special cases of a rigid and a free-surface sphere will it be the same. It can be shown[10] that in the former case $f_\infty\to\exp(-2ix)$ as x becomes large while for the free-surface sphere $f_\infty\to-\exp(-2ix)$. Hence, if the frequencies contained in the pulse are in the high frequency range, Eq. (14) becomes

$$P_r(\tau)=\frac{P_0}{2(2\pi)^{\frac{1}{2}}r_0^2}\int_{-\infty}^{\infty}g(x)\exp[ix(2R-2-\tau)]dx,$$

which means that the reflected pulse has the same form as the emitted pulse, but is returned time $2(r_0-a)/c$ later. This travel time indicates that the sound is reflected from a point source reflector at the point on the surface of the sphere nearest to the source of incident sound. A similar result holds for the free-surface sphere except that the pulse is inverted.

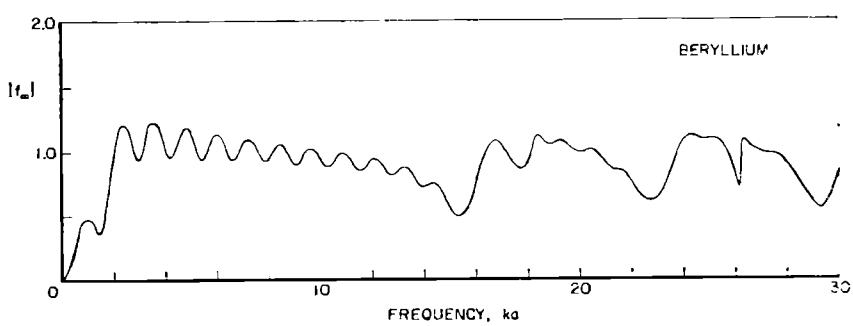

FIG. 3. The pressure amplitude as a function of frequency of the echo returned by a beryllium sphere to a distant source of continuous waves.

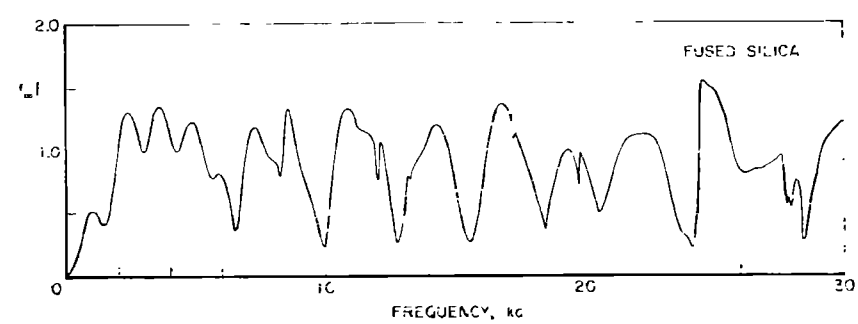

FIG. 4. The pressure amplitude as a function of frequency of the echo returned by a fused silica sphere to a distant source of continuous waves.

[10] Reference 3, p. 1554.

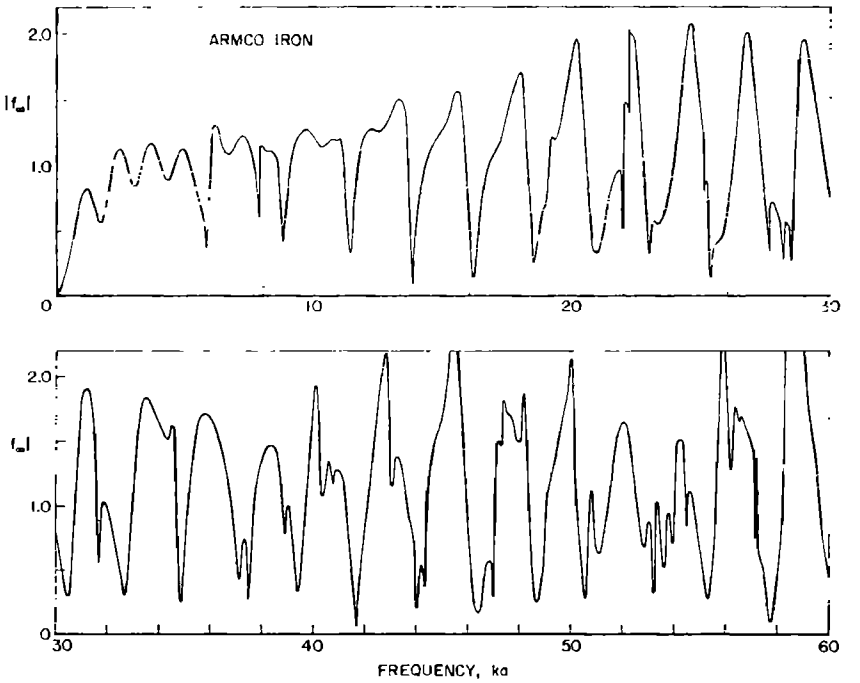

FIG. 5. The pressure amplitude as a function of frequency of the echo returned by a sphere of Armco iron to a distant source of continuous waves.

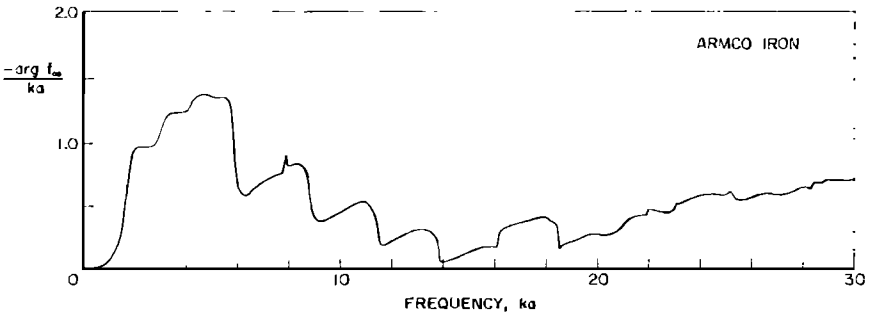

FIG. 6. The phase of the echo from the Armco iron sphere as a function of frequency.

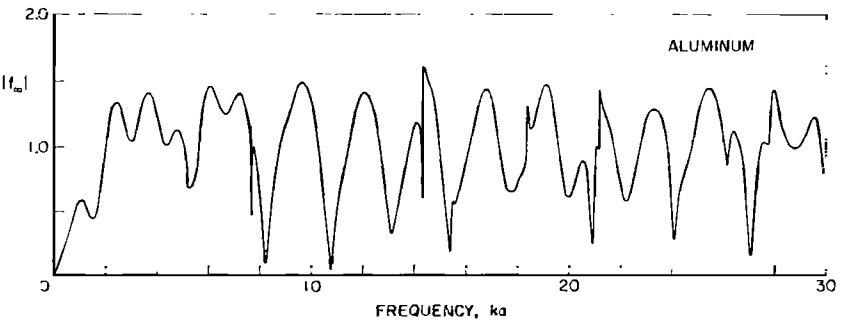

FIG. 7. The pressure amplitude as a function of frequency of the echo returned by an aluminum sphere to a distant source of continuous waves.

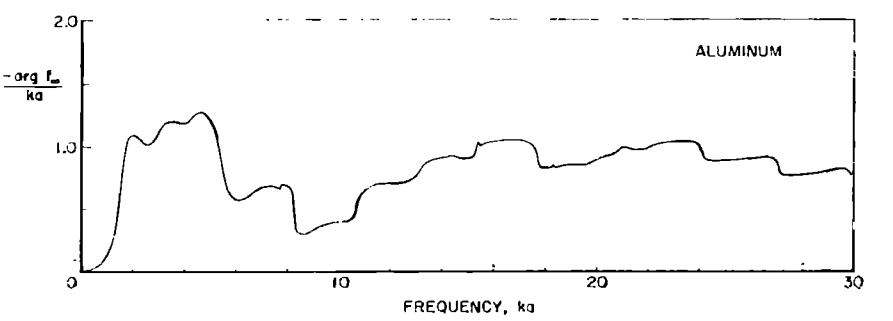

FIG. 8. The phase of the echo from the aluminum sphere as a function of frequency.

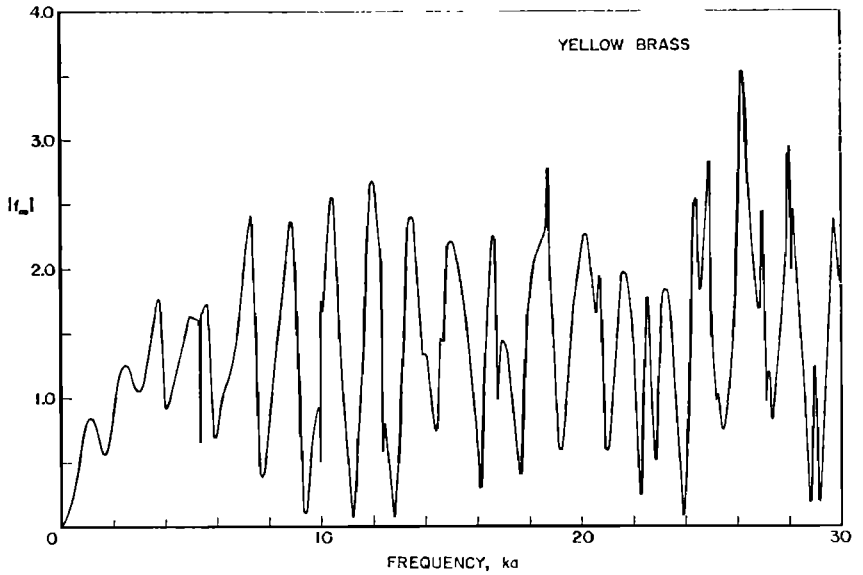

FIG. 9. The pressure amplitude as a function of frequency of the echo returned by a sphere of yellow brass to a distant source of continuous waves.

3. STEADY-STATE SOLUTIONS

The steady-state solutions given by the functions f in Eqs. (9), (10) were determined for a certain number of cases, the calculations being performed on a high-speed computer. The results are shown in Figs. 2–15.

The first results obtained were for the special cases of the rigid[8] and free-surface[9] spheres for a distant point source of continuous waves. These are shown in Figs. 2(a) and (b). The argument of the function f_∞ is presented divided by the variable $x=ka$. The results for the rigid sphere are in agreement with those of Stenzel.[5] For low frequencies the function is given by the initial terms in the series expansion which in the limit as x tends to zero are

$$\frac{2i}{x}\left[\frac{j_0'(x)}{h_0'(x)}-\frac{3j_1'(x)}{h_1'(x)}\right]\rightarrow 3x^2\left(1-\frac{ix^3}{3}\right),$$

and

$$(2i/x)[j_0(x)/h_0(x)]\rightarrow 2(1-ix),$$

for the rigid and free-surface spheres, respectively. For the rigid sphere this represents the well-known condition of Rayleigh scattering where the scattered intensity is proportional to the fourth power of the frequency. For the free-surface sphere the results are quite different. Not only does the scattered intensity reach maximum values at low frequencies, but the scattering is uniform in all directions. For high frequencies both solutions tend to the form $\exp(-2ix)$, the free-surface solution converging more rapidly than that of the rigid sphere. In the previous section, it was shown that this indicates

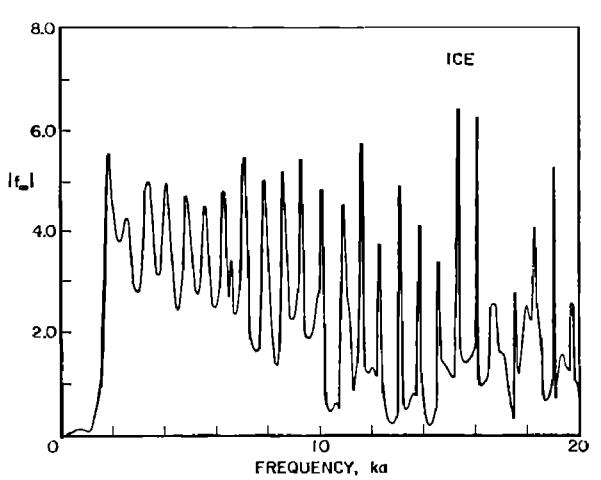

FIG. 10. The pressure amplitude as a function of frequency of the echo returned by an ice sphere to a distant source of continuous waves

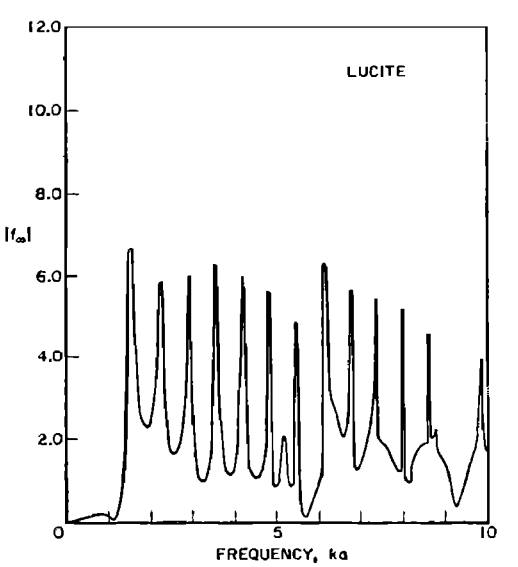

FIG. 11. The pressure amplitude as a function of frequency of the echo returned by a Lucite sphere to a distant source of continuous waves.

that at high frequencies the sound is mainly from a small area on the surface opposite the source and this would agree with physical intuition. At low frequencies the echo appears to come from the center of the rigid sphere and from a half-radius position in the free-surface sphere. As the frequency increases, the apparent origin of the echo moves gradually towards the region on the surface opposite the source. This is shown in Fig. 2(b), where the phase of f_∞ divided by $x=ka$ represents distance along a radius inside the sphere. In the case of the rigid sphere these results can be readily understood by supposing that low-frequency waves are intercepted by the entire cross section, whereas high-frequency waves behave as in geometrical optics and form a "bright spot" reflector on the surface opposite the source. With the free-surface sphere the results at low frequencies are not so readily explainable except that as expected they differ from those for the rigid sphere.

The main body of results were derived for solid spheres supporting internal shear and compressional waves. The properties of the materials considered are given in Table I. The fluid outside the sphere was assumed to be water of density 1 g/cc and compressional velocity 1410 m/sec.

As an initial test of the programs, the results obtained by Faran[2] were recalculated. Since these were for $\sigma=\frac{1}{3}$ no error could result from the misplacing of the factor $\sigma/(1-2\sigma)$ mentioned in the previous section since this factor is unity. Good agreement was found.

Some of the results for the materials listed in Table I are given in detail in Figs. 3–11. As before, these are for

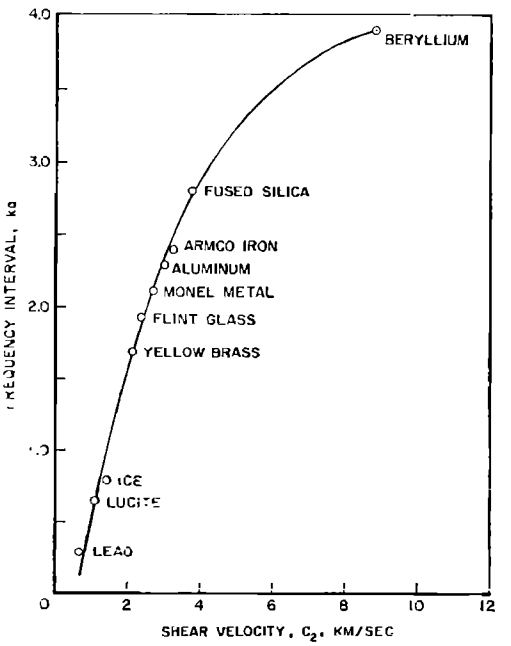

FIG. 12. Average interval in frequency between minima or between peaks in the pressure amplitude of the echo for different materials as a function of the shear velocity of the material

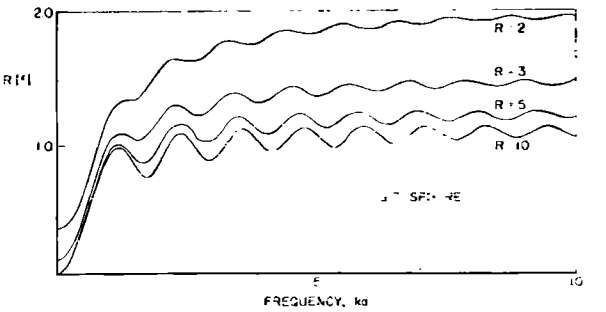

FIG. 13. The pressure amplitude as a function of frequency of the echo returned by a rigid sphere to a point source of continuous waves distance Ra from the center of the sphere.

a distant source. Generally the range of frequency was for values of ka up to 30, but for Armco iron, ice, and Lucite the range extended to $ka=60$, 20, and 10, respectively. In addition to the pressure amplitude the phase variation is given for Armco iron and aluminum. In all cases the results begin at low frequencies as though the solid were a rigid body, changing in general into a fairly regular series of peaks and minima as the frequency increases. With a rigid, incompressible material such as beryllium, the change from the rigid body solution is not very great. However, as the material becomes more compressible and pliant, the resonances tend to become more pronounced and more closely spaced. In the case of Lucite and ice the resonances have become quite sharp and close together. This general trend was investigated by considering an average frequency interval between minima or between resonance peaks for each material. The results are shown in Fig. 12 plotted against the shear velocity c_2. Parameters other than c_2 were also considered such as the Poisson's ratio, but with these the scatter of points was much greater. It appears therefore that this feature is most strongly dependent on the behavior of shear waves in the material. The successive peaks and minima which occur in the direct echo for a continuous frequency were shown by Faran[2] to be due to strong lobes of backscattered radiation forming and then splitting again into sidelobes

TABLE I.[a] Elastic constants.

Material	Density (g/cc)	Poisson's ratio σ	Compressional velocity c_1(m/sec)	Shear velocity c_2(m/sec)
Beryllium	1.87	0.05	12890	8880
Fused silica	2.20	0.17	5968	3764
Heavy silicate, flint glass	3.88	0.224	3980	2380
Armco iron	7.70	0.29	5960	3240
Monel metal	8.90	0.327	5350	2720
Aluminum	2.70	0.355	6420	3040
Yellow brass	8.60	0.374	4700	2110
Lucite	1.18	0.40	2680	1100
Lead	11.34	0.43	1960	690
Ice[b]	0.917	0.336	2743	1433

[a] *American Institute of Physics Handbook* (McGraw-Hill Book Company, Inc., New York, 1957).
[b] D. L. Anderson; Trans. Eng. Inst. Canada, 2, 116–122, (1958).

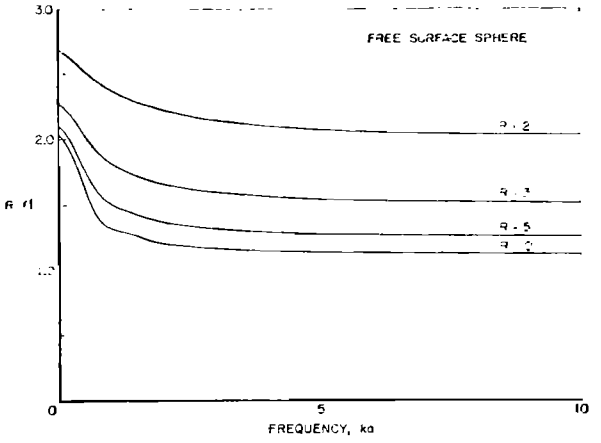

FIG. 14. The pressure amplitude as a function of frequency of the echo returned by a free-surface sphere to a point source of continuous waves distance Ra from the center of the sphere.

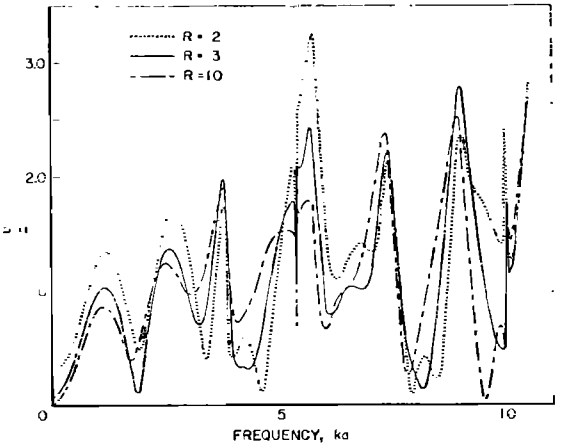

FIG. 15. The pressure amplitude as a function of frequency of the echo returned by a brass sphere to a point source of continuous waves distance Ra from the center of the sphere.

scattering in other directions. It seems therefore that shear waves play an important role in this process. Figs. 3–11 are arranged in order of decreasing shear velocity and a gradual process of transition seems to be apparent as this parameter is varied. As an independent parameter, the density of the material does not seem to have a very pronounced effect except at very low frequencies where the size of the first pressure-amplitude peak appears to vary in direct relation with it. As the frequency increases there appears to be no tendency towards some constant limit as in the cases of the free surface and rigid spheres. The peaks seem to recur, but in an increasingly ragged form.

In the phase variations shown in Figs. 6 and 8, jumps

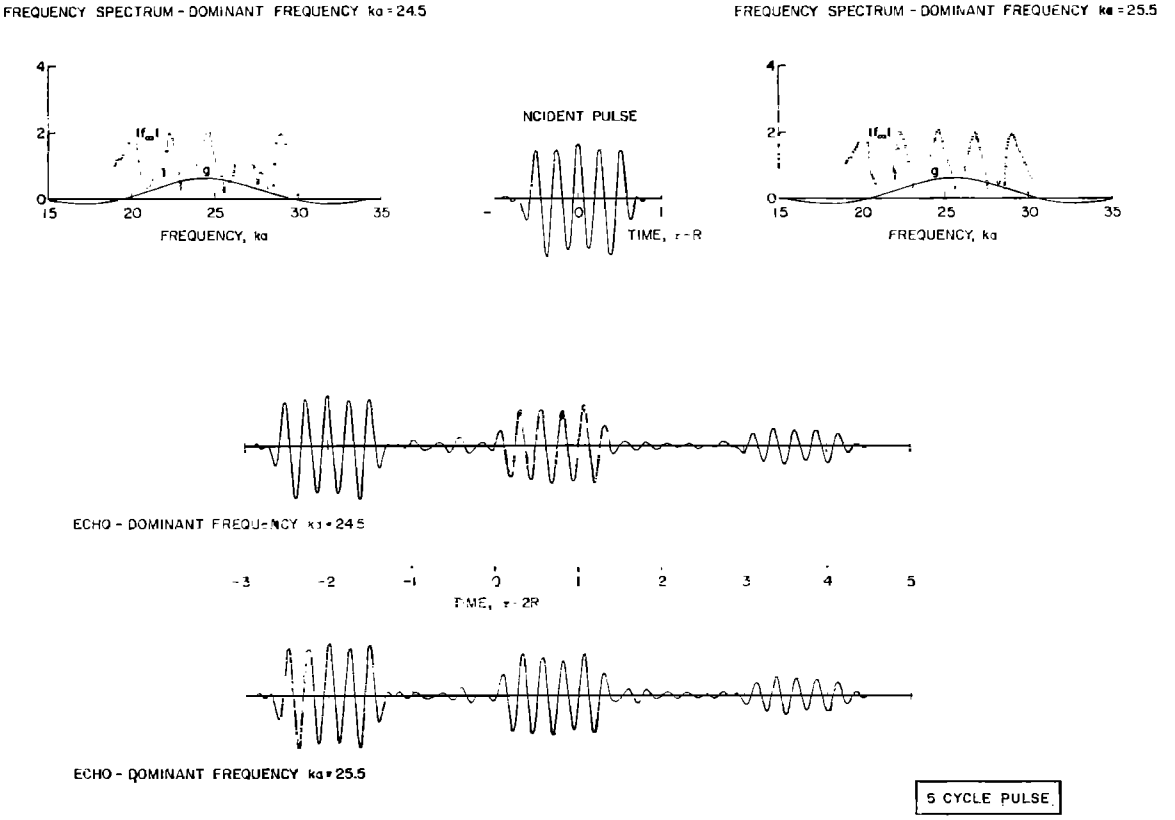

FIG. 16. Pulse forms of echoes returned by an Armco iron sphere for dominant frequencies at $ka = 24.5$ and 25.5 with an incident pulse of 5 cycles.

in phase occur at frequencies corresponding to minima in the pressure amplitude. As with the rigid body the parameter $(-\arg f_\infty/ka)$ is zero at the low-frequency limit and varies continuously as the frequency increases. Unlike the rigid sphere, however, this variation does not tend towards a limit where the apparent source of the echo corresponds to physical reality. The representation should therefore be regarded only as a convenient way of presenting the phase as a continuously varying function.

In order to determine the effect of distance of the sound source from the center of the sphere the function f in Eq. (9) was evaluated for a point source at various distances from a rigid, a free-surface, and a brass sphere. The pressure amplitude $|f|$ multiplied by R is shown in Figs. 13–15, allowing a ready comparison with the solutions for a distant source $|f_\infty|$. In general it appears that f_∞ represents a satisfactory solution when the sound source is situated more than 10 radii from the center of the sphere.

4. ECHO PULSE FORMS

The most obvious general feature in the steady-state solution for ordinary metals is the succession of peaks and minima in the pressure amplitude and it is of interest to determine how this affects the pulse form of the echo when the steady state solutions are used in the integral expression (14) for a distance source. The incident pulse form could be chosen arbitrarily. However, in practice the incident sound is generally produced by making a transducer resonate over several cycles at a particular frequency. Mathematically the pressure variation which results at a point in the fluid can be represented as follows:

$$\begin{aligned} P_i(t) &= 0, && t<-\Delta t,\\ &= \exp(-i\omega_0 t), && -\Delta t<t<\Delta t,\\ &= 0, && t>\Delta t, \end{aligned} \tag{15}$$

where ω_0 is the angular frequency of the transducer at resonance, and $2\Delta t$ is the duration of the pulse. The frequency spectrum $g(\omega)$ is given by the transform

$$g(\omega)=\frac{1}{2\pi}\int_{-\Delta t}^{\Delta t}\exp[i(\omega-\omega_0)t]\,dt$$
$$=(2/\pi)\sin[(\omega-\omega_0)\Delta t]/(\omega-\omega_0).$$

In the nondimensionalized system of Eq. (14) this becomes

$$g(x)=(2/\pi)\sin[(x-x_0)\Delta\tau]/(x-x_0), \tag{16}$$

where $x_0=\omega_0 a/c$ and is referred to as the dominant

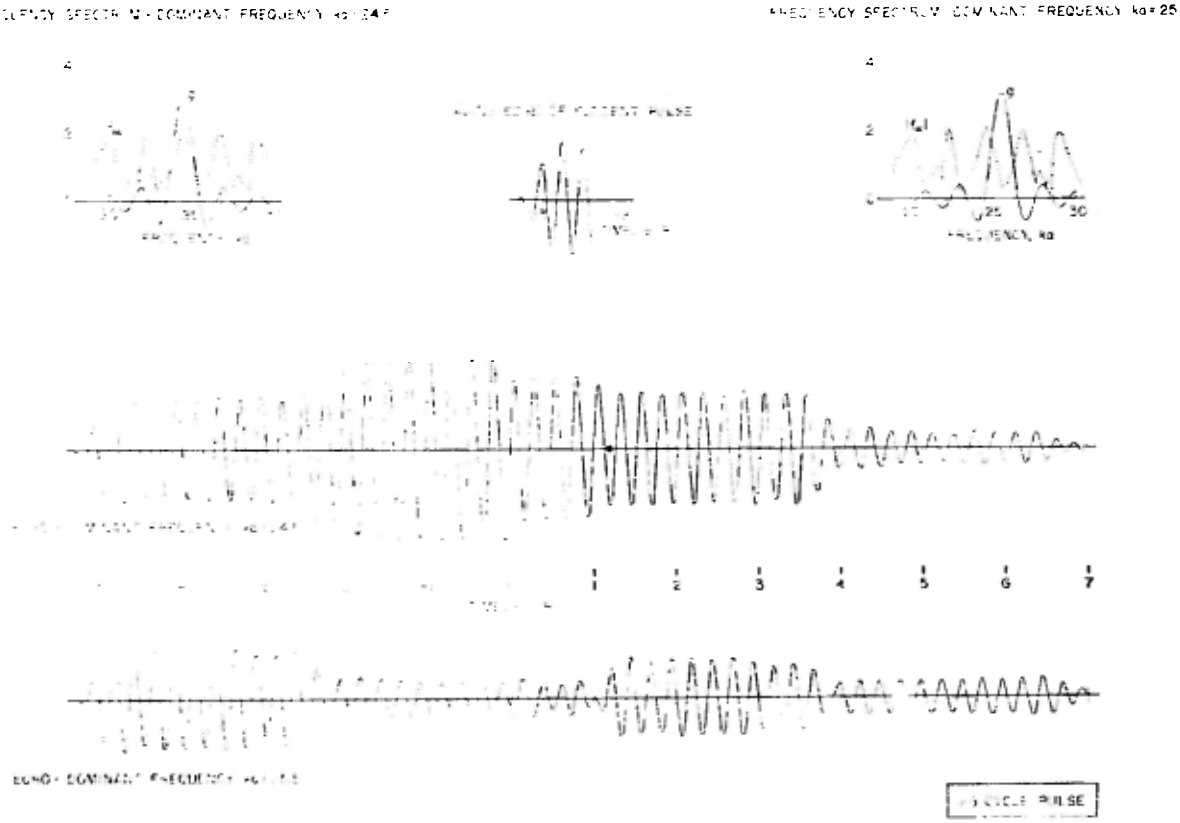

FIG. 17. Pulse forms of echoes returned by an Armco iron sphere for dominant frequencies at $ka=24.5$ and 25.5 with an incident pulse of 25 cycles.

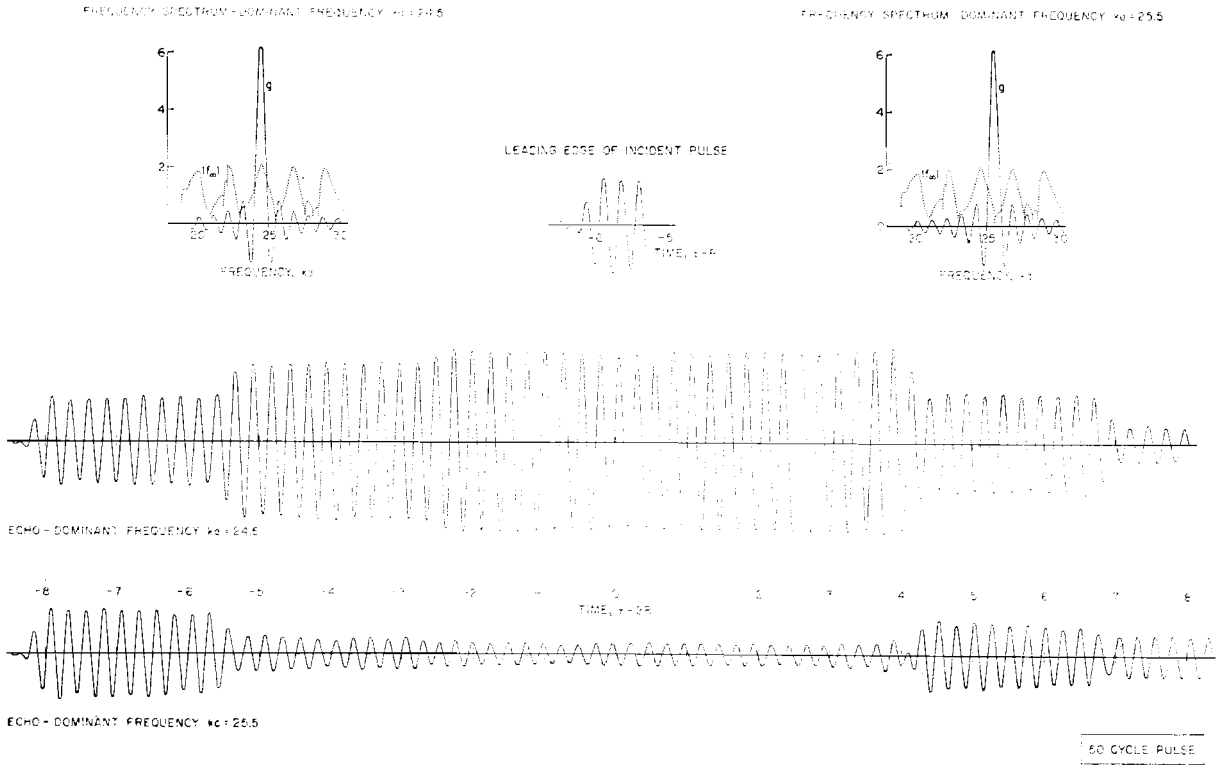

FIG. 18. Pulse forms of echoes returned by an Armco iron sphere for dominant frequencies at $ka = 24.5$ and 25.5 with an incident pulse of 50 cycles.

frequency. By use of Eq. (16) and the previously derived values of the function f_∞ it is then possible to obtain the pulse form of the echo by numerically integrating Eq. (14).

The nature of the function g in Eq. (16) is shown in Figs. 16–18 for different pulse lengths $\Delta\tau$. The height of the main peak occurring at the dominant frequency is equal to $\Delta\tau$ and its "spread" varies inversely with $\Delta\tau$. If the function $|f_\infty|$ is momentarily idealized as consisting of a series of similar, equally spaced peaks, it would appear that the form of the echo depends mainly on the pulse length and on the location of the dominant frequency relative to the maxima and minima of the $|f_\infty|$. Two extreme cases would then arise depending on whether the dominant frequency coincided with a maximum or with a minimum of $|f_\infty|$.

Using the data for Armco iron as shown in Figs. 5 and 6 several echo pulse forms were computed for different lengths of the incident pulse and for dominant frequencies corresponding to values of x or ka at 24.5 and 25.5. The former frequency occurs at a peak of the pressure amplitude and the latter at a minimum. The range of integration over ka for the longer pulses was from 15 to 35, while for the short 5-cycle pulse, it extended from 10 to 40. The incident pulse did not therefore have a perfectly rectangular form. However, in comparison to experimental pulse forms, it could be considered a satisfactory approximation. In addition the irregularities introduced by restricting the range of integration facilitated the recognition of certain features of the incident pulse in the echo. The calculated echoes are shown in Figs. 16–18. The time scale for the incident pulse is chosen with respect to the time of arrival of the midpoint of the pulse at the center of the sphere, whereas the scale for the echo is chosen with respect to the time of arrival back at the source. All pulses are shown traveling from right to left. It can be seen from these figures that the leading edge of the echo precedes that of the incident pulse by a time difference of 2 in each case. In addition the leading edge of the echo is of the same form as the leading edge of the incident pulse. These features indicate that the first part of the echo consists of a rigid body reflection from the region of the surface of the sphere adjacent to the sound source. The subsequent parts of the echo are affected by the vibrations of the sphere. In the case of the 5-cycle pulse, the first echo is of identical form to the incident pulse, while the second echo is also of the same form, but inverted. Subsequent echoes diminish in amplitude and lose the characteristic features of the incident pulse. Whether the dominant frequency occurs at a minimum or a maximum of the function $|f_\infty|$ does not appear to make much difference to the form of the echo for the short 5-cycle pulse, but obviously it is important when the pulse is longer. The reason can be seen from the frequency spectra shown in Figs. 16–18. A change in ka of the order of 1 in the spectrum for the short pulse will not greatly affect the integral (23); however, this is not

the case for the longer pulses. The differences in form of the echoes shown in Figs. 17, 18 are in fact quite distinctive. It seems, moreover, that the changes which occur when the dominant frequency is moved from a maximum of $|f_\infty|$ to a minimum, are characteristic of any ordinary metal. Figure 19 shows the echoes from a sphere of aluminum for the same type of incident pulse, where these results were obtained experimentally.[1] With allowance for a change of scale and such effects as the response of the transducer, the differences in the echo resulting from a change in the dominant frequency are closely related to those shown in Figs. 16–18. The sphere in this case had a diameter of 5 in. and the change in dominant frequency was from 120 to 123.5 kc/sec. This is equivalent to a change in ka of about 1, which according to Fig. 12 is the approximate distance between a peak and a minimum of the function $|f_\infty|$ for most metals including aluminum. Using the constants given above for water and aluminum, it is found that 120 kc/sec does not in fact coincide with a peak of the steady-state reflection function $|f_\infty|$. However, this is not surprising, since the values used referred to rolled aluminum. In addition if the frequency is to be expressed in terms of ka with any accuracy, it would be necessary to know the velocity of sound in water under the conditions of the experiment, and also the diameter of the sphere, to within less than 1%. Echoes were calculated for rolled aluminum at values of ka equal to 34.6 and 35.6 corresponding to frequencies of 122.3 and 125.8 kc/sec, the values occurring at a maximum and a minimum, respectively, of the reflection function $|f_\infty|$. The pulse lengths $\Delta\tau$ were the same as those in Figs. 16–18. Similarly, echoes were calculated for a brass sphere for frequencies at $ka=20.2$ and 21.0. These echoes were found to have the same features. The leading edge was a rigid body reflection and the same kind of transition in pulse form occurred when the frequency and the pulse length were varied. With yellow brass the secondary echoes in the multiple echo forms had a bigger amplitude than the primary echo.

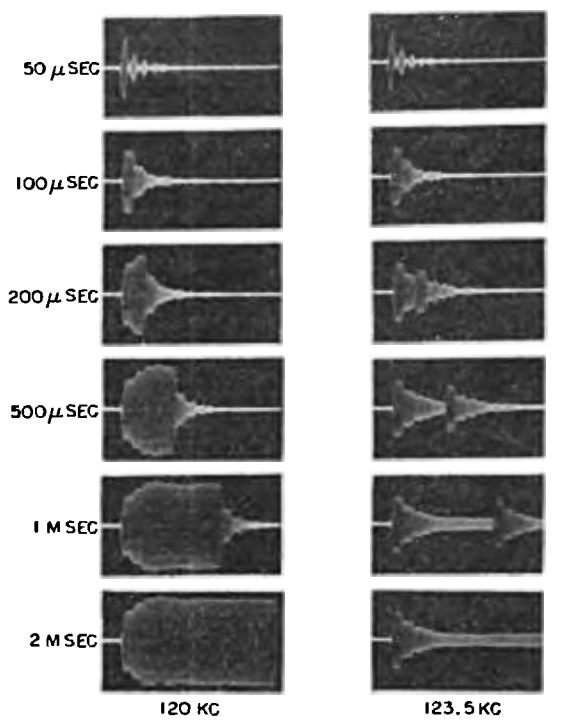

FIG. 19. Experimentally determined echo forms for a 5-in.-diameter aluminum sphere for various incident pulse lengths. The sweep is 150 μsec/cm.

5. DISCUSSION

Although this paper represents only a preliminary study, it may be worthwhile to consider the significance of the results in relation to the problem of using sonar echoes to obtain information about a target.

In the first place, it would seem that solid materials could be divided roughly into two groups, metallic flint-like substances and substances which are fairly pliant. This can be seen from the steady-state solutions, where the former is characterized by a succession of peaks and minima roughly the same distance apart, while the latter has sharper, stronger peaks more closely spaced. Although all the echo forms which were calculated belong only to the first type, it is evident from the steady-state solutions that there would be a difference in the general nature of echoes between the two groups. Hence there would exist the possibility of distinguishing, for instance, between a bare rock and a large fish.

Secondly, if the sonar target is known to be a homogeneous metallic sphere, then it is possible to determine its approximate radius by using data of the type shown in Fig. 19. The features of the transition between a peak and a minimum of the steady-state reflection function $|f_\infty|$ for the long incident pulses is characteristic of most ordinary metals, as shown in the previous section. The transition is accomplished during a change in ka of the order of 1. Hence given an actual change in frequency in cycles per second, it is then possible to determine the radius a of the sphere. For example, the transition in pulse form shown in Fig. 19 is achieved through a frequency change of 3.5 kc/sec corresponding to a change in ka of about 1 which therefore makes the radius of the sphere approximately 2.5 in. In general, however, such an estimate would not be quite so accurate. It also seems possible to estimate the size of the sphere by varying the pulse length rather than the frequency, since the individual echoes occurring in the short pulse become contingent when the incident pulse length is approximately equal to the diameter of the sphere (see Fig. 19).

Finally, it has been shown[11] that there are significant differences in the steady state reflection function f_∞ for rigid bodies of different shapes. Although these effects would be rendered more complicated by allowing for the

[11] R. Hickling, J. Acoust. Soc. Am. 30, 137–139 (1958).

vibrations of the solid material, it may be possible to use them to derive some information about the shape of a sonar target.

ACKNOWLEDGMENTS

The author is grateful to Professor M. S. Plesset for helpful encouragement of this work and to Professor T. K. Caughey for several useful discussions. He is also greatly indebted to Dr. Chester M. McKinney for permission to reproduce some of his experimental results. Some of the computations were performed at the Western Data Processing Center at the University of California in Los Angeles. This study was supported by the Office of Naval Research.

THE JOURNAL OF THE ACOUSTICAL SOCIETY OF AMERICA VOLUME 34, NUMBER 10 OCTOBER 1962

Surface Backscattering Strengths Measured with Explosive Sound Sources

R. P. CHAPMAN AND J. H. HARRIS
Naval Research Establishment, Dartmouth, Nova Scotia, Canada

(Received June 12, 1962)

The scattering strength of the sea surface was measured for a range of wind velocities, grazing angles, and frequencies, in octave bands in the frequency range from 400 to 6400 cps. An empirical equation was obtained relating the scattering strength of the sea surface to the above variables, for grazing angles below 40°. At low grazing angles, scattering of sound from a subsurface layer of isotropic scatterers, probably of biological origin, frequently masked the reverberation due to scattering from surface roughness. For a given wind speed, the scattering strengths measured in this study at grazing angles below 20° were appreciably less than those obtained by other observers at higher frequencies. At higher grazing angles, of the order of 40°, there was little systematic difference between the measurements made at high and low frequencies.

INTRODUCTION

A NUMBER of systematic studies of the backscattering of sound from the sea surface have been carried out at frequencies of tens of kilocycles per second,[1,2] but none has been reported for low frequencies. This report describes an investigation designed to measure the variations of surface scattering strength with wind velocity, grazing angle, and frequency, in octave bands in the frequency range from 400 to 6400 cps. A number of characteristics of the surface scattering process are discussed and an empirical relationship obtained relating surface scattering strength to wind velocity, frequency, and grazing angle. At low grazing angles, the scattering strengths tended to become independent of grazing angle. This arose because the sound, scattered from the sea surface at the longer ranges, was masked by the scattering of sound from a layer of isotropic scatterers, probably of biological origin, in the volume of the sea.

SEA TRIALS AND ANALYSIS

The sea trial was carried out over a 52-h period in March 1961 in deep water north of Bermuda (35°N, 65° W). The water was isothermal from the surface to at least 1200 ft. During the trial, in which reverberation measurements were made at random times between 9 a.m. and midnight, the winds, measured on the ship's anemometer, ranged from zero to 30 knots, and the sea was estimated to range from zero to state 6.

Measurements of reverberation were made with an omnidirectional hydrophone connected by an armored cable to a magnetic tape recorder on the ship. Suspended below the hydrophone, five 1-lb charges of TNT were spaced at 5-ft intervals. The charges were detonated at 1-min intervals after being lowered to the desired depth. Experiments were carried out with the hydrophone at nominal depths of 300, 600, and 1200 ft.

The recordings were played back through octave band filters and the output displayed on a logarithmic Sanborn recorder. The scattering strengths at various times after the explosion were obtained from these recordings using the following equation derived in Appendix I:

$$10\log S = 20\log P - 10\log E + 30\log t - 42, \qquad (1)$$

where $10\log S$ represents the scattering strength of the sea surface; $20\log P$ represents the contribution to the experimental reverberation levels, in decibels relative to 1 dyn/cm², in the band considered due to the shock pulse at a time t after the explosion. At frequencies above 800 cps, the bubble pulse energy made an insignificant contribution to the measured reverberation level. In the 400–800 cps band, corrections of from 1 to 3 dB had to be made to allow for the contributions of

[1] R. J. Urick and R. M. Hoover, "Backscattering of Sound from the Sea Surface; Its Measurement, Causes, and Application to the Prediction of Reverberation Levels," J. Acoust. Soc. Am. 28, 1038 (1956).

[2] G. R. Garrison, S. R. Murphy, and D. S. Potter, "Measurements of the Backscattering of Underwater Sound from the Sea Surface," J. Acoust. Soc. Am. 32, 104 (1960).